INFLUENCE OF PRECIPITATION ON BRANCHED CRACK FORMATION IN SURFACE ZONE OF CONTINUOUSLY-CAST SLABS OF Ti-Nb HSLA STEEL

BEKEČ Pavel [1,2], LONGAUEROVÁ Margita [2], LONGAUER Svätoboj [2], MILKOVIČ Ondrej [2], KONRÁDYOVÁ Jana [2], TRÉFA Gabriel [3], GRIMPLINI Gabriel [3]

[1]ŽP Research and Development Centre, Podbrezová, Slovakia, EU, bekec@zelpo.sk
[2] Technical University of Kosice, Department of Materials Science, Kosice, Slovakia, EU
[3] U.S.STEEL Kosice, Ltd., Research and Development Centre, Košice, Slovakia, EU

Abstract

This work studies the influence of precipitation on branched crack formation in the surface skin of continuously-cast slabs of Ti-Nb HSLA steel. Two slabs were analysed, cast at pulling rates of 0.43 m.min^{-1} and 1.03 m.min^{-1}. The results show that branched cracks were located on the slab with pulling rate 0.43 m.min^{-1}, which was a transition slab. The branched cracks extended to a depth of 10 mm below the slab surface and occurred mostly below oscillation marks. In the case of the slab cast at pulling rate 1.03 m.min^{-1} branched cracks did not occur. Evaluation of precipitates obtained by the method of carbon extraction replicas on selected samples confirmed the presence of predominantly spherical or elliptical particles. Square particles were observed in small amounts. Application of selection electron diffraction showed the presence of TiC and NbC carbides. Formation of cracks is influenced by the size of precipitate particles, but also by morphology and distribution of precipitates. It is known that elliptical precipitates have significantly worse effects than spherical precipitates, even when significantly smaller and fewer in number. Globular particles also influence formation of surface cracking, but only when they occur in steel at high volumes or very large size. It is also known that precipitates arranged in rows on grain boundaries cause surface cracking. In this work the slab cast at the lower pulling rate 0.43 m.min^{-1} showed the presence of adverse precipitates and also rows of excluded precipitates on grain boundaries, which were considered responsible for the observed branched cracks. The formation of branched cracks is conditioned not only by segregation of impurities, but possibly also by the presence of undesirable brittle cementite networks. The presence of cementite was confirmed not only through microstructural analysis, but also diffraction of hard X-ray radiation. This diffraction revealed a branched crack in the sample cast at pulling rate 0.43 m.min^{-1} including the presence TiC and Fe_3O_4, the amounts of which were comparable to the amount of Fe_3C in the analyzed area. On a sample without occurrence of branched cracks at pulling rate 0.43 m.min^{-1}, there was only Fe_3C in detectable amounts. It is known that precipitation of microalloying elements in connection with cementite can lead to higher probability of surface crack formation, as also confirmed in this study.

Keywords: Slab, branched cracks, oscillation marks, segregation, precipitation

1. INTRODUCTION

Particle precipitation with microalloying elements in continuously-cast slabs can influence microstructure during further processing, e.g. reheating and after the hot rolling process. Therefore, it is necessary to study precipitation not only in the hot rolling process, but also in the cast state. According to the authors of works [1,2] microsegregation during the casting process can result in non-uniform distribution of precipitates with Ti and Nb in continuously-cast slabs, which can cause changes in the austenite grain size during heating. During continuous casting precipitates may be formed during solidification. Their formation during the continuous casting is very strongly influenced by solidification of the slab and cooling of the crystallizer, the secondary cooling zone and cooling outside of the casting machine. The presence of precipitates based on microalloying elements or impurities can adversely influence the quality of continuously-cast products, especially in terms of formation of surface cracks. Therefore it is importa20nt to understand the rules of precipitate formation during

continuous casting, in order to avoid degradation of products. According to work [3] the morphology of precipitates affects surface cracking in continuously-cast semi-finished products. This work builds on work [4], where the aim was to study the background of branched crack formation in a continuously-cast slab made from Ti-Nb microalloyed steel in terms of structural, chemical and phase analysis. The aim of this work is to show the influence of the distribution and morphology of precipitates on the formation of branched cracks in the surface area of the transition slab.

2. MATERIAL AND EXPERIMENTAL METHODS

A transition slab of Ti-Nb microalloyed steel cast with initial pulling rate 0.43 m.min^{-1} and final rate 0.9 m.min^{-1} and a slab cast at the real pulling rate 1.03 m.min^{-1} were compared. **Tables 1** and **2** show the chemical composition of the analysed slabs. Cut-outs were taken for analysis from the transition slab towards its slower cast end, i.e. 0.43 m.min^{-1}, as shown in **Fig. 1**. From the slab cast at the real pulling rate cut-outs were taken as shown in **Fig. 2**, while marginal cut-out U was not available. Samples were taken from the individual cut-outs for evaluation of particles. The samples were taken parallel to the slab pulling direction and perpendicular to the slab surface. The analyzed area consisted of about 20 mm^2. In the case of the slab cast at pulling rate v = 0.43 m.min^{-1} samples A36 and A37 were taken from marginal cut-out A . The surface zone analyzed was about 5 mm below the slab surface in sample A36, and 9 mm deep in sample A37. The surface of sample A36 was characterized by the presence of oscillation marks (OM) about 2 mm deep and branched cracks below OM about 6 mm long. From central cut-out B sample B31 was taken, the evaluated area reaching about the depth of 4 mm below the slab surface. In the case of the slab cast at the real pulling rate v = 1,03 m.min^{-1} sample R26 was taken from marginal cut-out R, while the particles were analyzed in the slab surface zone to a depth of about 3 mm from the slab surface. From central cut-out S sample S33 was taken, and the particles were analyzed to a depth of about 4 mm below the slab surface.

Table 1 Chemical composition of the transition slab (wt.%)

C	Mn	Si	P	S	Al	Mo	Ti	V
0.082	0.899	0.011	0.011	0.007	0.033	0.002	0.012	0.001
Nb	**N_2**	**Cu**	**Ni**	**As**	**Sn**	**Zr**	**Cr**	**B**
0.035	0.0061	0.032	0.014	0.004	0.009	0.001	0.014	0.0002

Table 2 Chemical composition of the slab cast at the conventional pulling rate 1.03m.min^{-1} (wt.%)

C	Mn	Si	P	S	Al	Mo	Ti	V
0.079	0.532	0.012	0.009	0.005	0.033	0.002	0.017	0.002
Nb	**N_2**	**Cu**	**Ni**	**As**	**Sn**	**Zr**	**Cr**	**B**
0.025	0.004	0.039	0.01	0.001	0.002	0.016	0.016	-

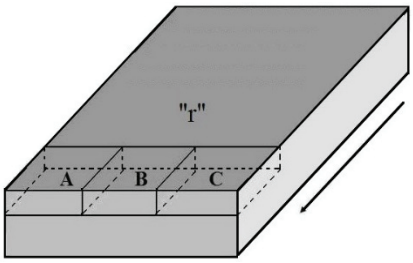

Fig. 1 The cut-out positions and pulling direction of the transition slab (v = 0.43 m.min^{-1})

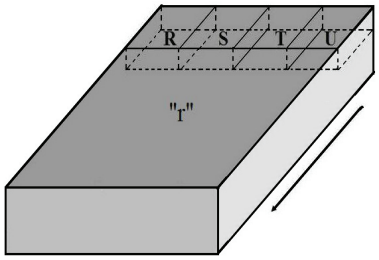

Fig. 2 The cut-out positions and pulling direction of the conventional slab (v = 1.03 m.min^{-1})

Transmission electron microscopy (TEM) on a JEOL JEM 2000 FX microscope was used to evaluate precipitates (size, shape, distribution) in selected samples from the individual cut-outs. Patterns were identified using diffraction in particles obtained from carbon extraction replicas. Preparation of samples for the replicas consisted firstly of mechanical grinding and polishing and later also electrolytic polishing in electrolyte with the following components: acetic acid - CH_3COOH (100 %) and perchloric acid $HClO_4$ (70 %), in the ratio 9:1. For etching 2 % Nital was applied followed by vaporizing with carbon. Replicas were electrolytically separated in 4 % Nital. Statistical evaluation of the size of the precipitates in selected samples was carried out as follows: the density and distribution of precipitates were visually evaluated in several images, then the linear dimension of the particle 2r was determined from images of the replicas, and the number of precipitates for each dimension was found. The measured numbers of precipitates in the samples were different, ranging in the interval 171 - 686 precipitates. By recalculation the relative frequency of particles N was determined, as well as the mean size of the particles. The final method used was diffraction of hard X-ray radiation, carried out at the experimental station on P02.1 localized on the PETRA III positron accelerator at HASYLAB/DESY in Hamburg. Sample C12 with a crack in the surface zone from marginal cut-out C (v = 0.43 $m.min^{-1}$) was used for analysis. By grinding to a depth of 2 mm from the slab surface and the underside of the samples as well, the final thickness of the sample intended for diffraction analysis reached ~ 1 mm. Hence diffraction analysis was performed in effect at a depth of ~ 2 mm below the slab surface. Sample T10 without cracks in the surface area was similarly prepared from central cut-out T (1.03 $m.min^{-1}$). The beam of photons was directed as in the case of sample C12 (0.43 $m.min^{-1}$) to pass through the area of the crack. Samples were irradiated for a period of 20 seconds by photon beam with energy of 58 keV (λ = 0.207271 Å) with an effective cross section of 0.5 x 0.5 mm^2. The diffractive image was recorded with a Perkin Elmer 1621 2D detector and subsequently integrated into the dependence of intensity-angle (2Θ) using FIT2D software. The distance of the detector from the sample, orthogonal deposition of the detector towards the beam, determination of the center of the detector, as well as calculation of the energy of radiation, were all effected by measuring the reference sample CeO_2.

3. RESULTS

Sample A36 with a branched crack was taken from marginal cut-out A (v = 0.43 $m.min^{-1}$). From this sample particles were extracted from surrounding cracks under deep OM and transformed into carbon replicas. In the sample 226 particles in total were counted. Their size ranged from 4.6 to 76.9 nm. Most of the particles were within the range 10 - 19 nm, and their share was 51.3%. Only 3 particles had a size of ~ 76.9 nm. Particles occurring in this zone were relatively fine, and their average size was 18.9 nm. They had mostly globular or ellipsoidal shape, and square particles were rarely observed. Distribution of the particles was non-uniform, though in places predominantly globular particles were observed excluded in a row, as demonstrated in **Fig. 3**. Using selection electron diffraction carbides of titanium and niobium were identified, namely TiC and NbC. Particles from a place below OM were analyzed in the second sample A37 from marginal cut-out A, as well as the occurrence of cracks in the surface zone further below the slab surface (~9 mm). From this sample in total 285 particles were evaluated, with sizes ranging from 8.8 to 79.4 nm. The particles were predominantly relatively fine (30 nm), but particles with larger sizes (over 50 nm) also occurred. In general these particles were larger compared to the previous sample A36. 56.1% of the particles were sized in the range 20-29 nm. Their average size was 23.8 nm. They were mostly globular in shape, but elliptical and square ones also occurred. The particle distribution was non-uniform (**Fig. 4**). In sample B31 taken from central cut-out B (v = 0.43 $m.min^{-1}$), particles from the surface zone below shallow OM were evaluated. Most of the particles were very fine, and most of them were globular, only some elliptical, and these particles were also non-uniformly distributed (**Fig. 5**). A total of 686 particles with sizes ranging from 5.6 to 41.2 nm were measured. Most represented were the finest particles in the range of 1-9 nm, namely 54.1%. Using circular diffraction evaluation the presence of titanium carbide TiC was confirmed. The average size of the particles in the sample was 10.9 nm.

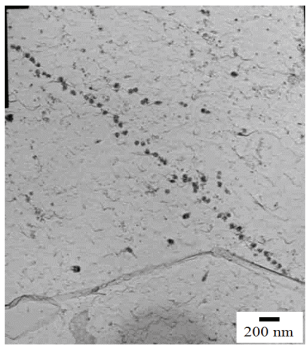

Fig. 3 Particles excluded in a row, sample A36, v = 0.43 m.min^{-1}

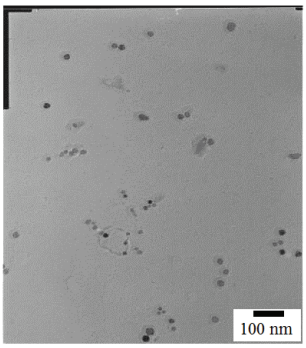

Fig. 4 Fine particles, sample A37, v = 0.43 m.min^{-1}

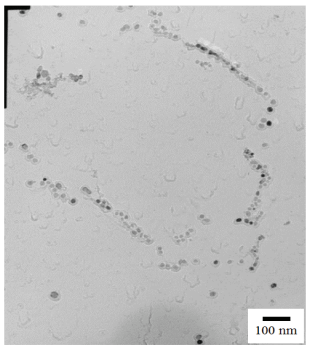

Fig. 5 Non-uniform distributed fine particles, sample B31, v = 0.43 m.min^{-1}

Taken from the slab cast at the real pulling rate 1.03 min^{-1} without occurrence of branched cracks on the surface, sample R26 from marginal cut-out R was analyzed. Particles were analyzed from the slab surface zone to a depth of 3 mm. The particles were globular, elliptical, square and occasionally were observed also in the shape of a cross (**Fig. 6**). A total of 177 particles were evaluated. Their size reached values ranging from 14.3 to 116.7 nm. Most represented were particles in the range 30 - 39 nm. This proportion was 31%. Particles over 50 nm also occurred in larger numbers. The average size of the particles was 43.2 nm. Their distribution was non-uniform and most were sparsely excluded (**Fig. 6**). Occasionally particles excluded in a row were observed. In sample S33 from the central cut-out of the slab cast at v = 1,03 m.min^{-1}, particles from the surface zone were analyzed. The particles in this sample were coarse compared with those from samples at the lower pulling rate. 171 particles were evaluated. Their sizes ranged from 19 to 112.5 nm. Most of the particles reached sizes in the range 40-70 nm, the greatest number being found in the range of 40 to 49 nm in the proportion of 34.5%. Two particles were larger than 100 nm. The particles were globular, elliptical, but also square. The distribution of particles was non-uniform, and areas was observed where the particles were excluded sparsely (**Fig. 7**), but also an area where the particles were excluded densely (**Fig. 8**). Average diameter of the particles was 51 nm, which is the largest average particle size from all the analyzed samples.

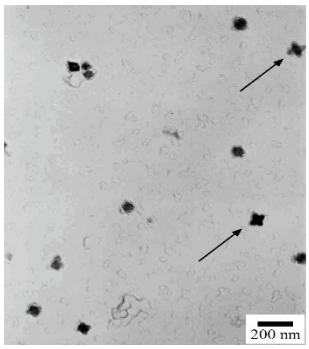

Fig. 6 Sparsely excluded particles + cross-shaped particles, sample R26, v = 1.03 m.min^{-1}

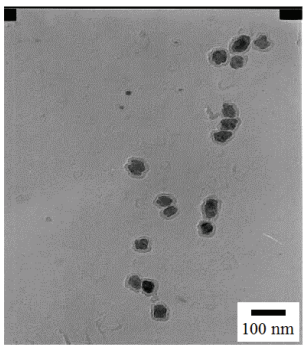

Fig. 7 Sparsely excluded particles, sample S33, v = 1.03 m.min^{-1}

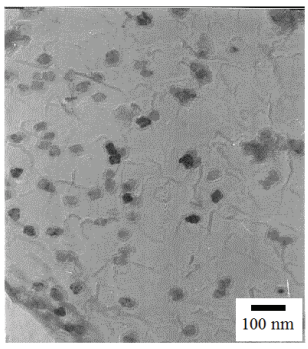

Fig. 8 Densely excluded particles, vzorka S33, v = 1.03 m.min^{-1}

The method of hard X-ray diffraction using the PETRA III positron accelerator at HASYLAB/DESY in Hamburg produced diffraction pattern sample C12 with cracks (v = 0.43 m.min^{-1}) and sample T10 without cracks (v = 1.03 m.min^{-1}), which showed that the indexed reflecting planes belonged in the majority phase of α-Fe, while the minor phase was almost unidentifiable. In spite of the fact that the software did not identify the minor phase, the reflections are situated in the detailed diffraction records that are shown in **Fig. 9** and **Fig. 10**. The record sample C12 identified a total of three secondary phases: Fe_3O_4, TiC and Fe_3C. For phase analysis more than 20 standards were compared, including inclusions which may be present in the steel. The compared standard

phases responded with very accurately identified peaks, and the amounts of TiC and Fe_3O_4 were comparable to that of Fe_3C in the analyzed area. In sample T10 the Fe_3C phase was identified, i.e. in this steel only cementite occurs in detectable amounts.

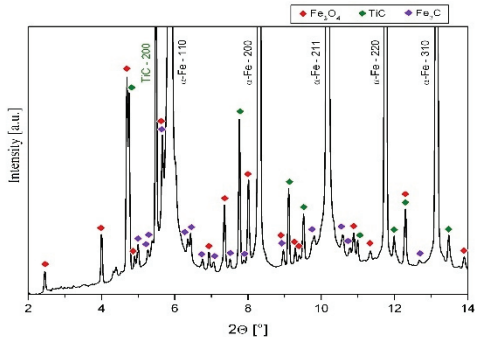

Fig. 9 Detail of diffraction record of sample C12 (v = 0.43 m.min^{-1})

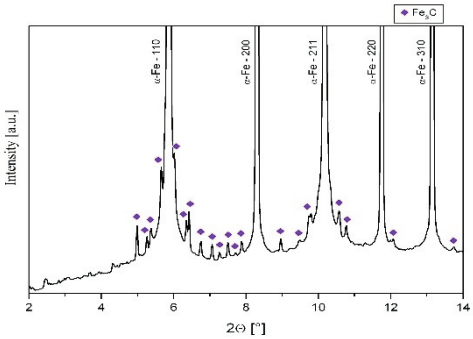

Fig. 10 Detail of diffraction record of sample T10 (v = 1.03 m.min^{-1})

4. DISCUSSION

Macroscopic analysis showed that in the analyzed surface zone of the slab no visible surface defects occurred. In the slab surface cast at the lowest pulling rate v = 0.43 m.min^{-1} OM of varying depth were observed, while after the taking of test samples and grinding the surface of the slab the occurrence of branched cracks was demonstrated. They were mostly below the OM. In the case of the slab cast at the real pulling rate v = 1.03 m.min^{-1}, no OM or cracks were present. Evaluation of precipitates obtained from extraction replicas in selected samples confirmed the occurrence of predominantly globular or elliptical particles. Square particles were observed in small amounts. Using selection electron diffraction we identified carbides (TiC and NbC). In the case of the slab cast at the lower rate v = 0.43 m.min^{-1} the particles were smaller than those found in the slab cast at the real rate v = 1.03 m.min^{-1}. At casting rate v = 0.43 m.min^{-1} average particle sizes of 18.9 nmand 23.8 nm respectively were found in locations with cracks, whereas at the rate v = 1.03 m.min^{-1} the average particle sizes were larger, namely 43.2 and 51 nm respectively. The morphology of the precipitates according to work [3] affect surface cracking in continuously-cast products as follows. The precipitates of globular shape influence the occurrence of surface cracks only when they are contained in steel at high volumes and they are large. Precipitates excluded in a row at the original grain boundaries, no matter what their shape, probably cause surface cracking just like precipitates on the secondary grain boundaries. Precipitates excluded in a row were observed in the transition slab with the occurrence of cracks at pulling rate v = 0.43 m.min^{-1} (**Fig. 3**). Elliptical precipitates are significantly worse than globular precipitates, even when significantly smaller and in smaller numbers. Small elliptical precipitates were seen in greater amounts only at the lower pulling rate v = 0.43 m.min^{-1} in contrast to the real pulling rate v = 1.03 m.min^{-1}. Cuboid or rod-shaped precipitates also influence the formation of surface cracks, even in small amounts. As can be seen in the diffraction record detail in **Fig. 9**, three phases were identified in sample C12 with a crack from marginal cut-out C (v = 0.43 m.min^{-1}), namely Fe_3O_4, TiC and Fe_3C. The amounts of TiC and Fe_3O_4 were comparable to that of Fe_3C in the analyzed area. In the detail of the second diffraction record of sample T10 without a crack (v = 1.03 m.min^{-1}), Fe_3C was identified only in detectable amounts. According to the authors of [3], Fe_3C in connection with particle precipitation with microalloying elements, results in increased probability of surface crack formation. This was also confirmed in this study, since Fe_3C and also TiC were identified in sample C12 with a crack. Formation of branched cracks in the surface skin of the analyzed slab made from Ti-Nb microalloyed steel in the case of lower pulling rate 0.43 m.min^{-1} is due to a combination of several factors. It is due to the lower pulling rate, because at this rate longer time is available during segregation processes [5]. Intensive development of segregation processes at the lower slab pulling rate was confirmed in work [4], where local accumulation of sulphur at a concentration of up to 1.17% was confirmed, as well as high content of surface-active elements

at a concentration of up to 0,26%. Last but not least, work [4] confirmed the presence of intercrystalline facets on fractures obtained by opening of branched cracks, also showing the segregation of harmful impurities and precipitation at the original austenite grain boundaries, which weakens their cohesion strength.

5. CONCLUSIONS

Study of the influence of particle precipitation on branched crack formation in continuously-cast slabs of Ti-Nb microalloyed steel leads to the following conclusions:

1) On the slab cast at the lower pulling rate (v = 0.43 m.min^{-1}) the presence of branched cracks was detected in the surface skin, extending to a depth of 10 mm and mostly occurring below the OM. On the slab cast at the real pulling rate 1.03 m.min^{-1}, branched cracks did not occur.
2) Using selection electron diffraction on samples from the slab surface zone were identified carbides (TiC a NbC). The precipitates were smaller, with average size of 18.9 nm at the lower slab pulling rate v = 0.43 m.min^{-1} compared to the average size of the precipitates of 43.2 nm in the slab with real pulling rate v = 1.03 m.min^{-1}. The effect of the morphology of precipitates was demonstrated on the formation of branched cracks in the transition slab cast at the slower pulling rate v = 0.43 m.min^{-1}. The morphology effect was confirmed only in this slab by a larger share of adverse elliptical precipitates and precipitates arranged in rows compared to the slab without cracks at the real pulling rate 1.03m.min^{-1}.
3) The results of positron accelerator measurement of samples C12 with cracks (v = 0.43 m.min^{-1}) and T10 without cracks (v = 1.03 m.min^{-1}) showed that in sample C12 in addition to the majority phase of α-Fe three phases other were identified, namely Fe_3O_4, TiC and Fe_3C, while the amounts of TiC and Fe_3O_4 were comparable to that of Fe_3C in the analyzed area. In sample T10 without cracks only Fe_3C phase was identified. The presence of cementite in connection with precipitation of microalloying elements can lead to higher probability of surface crack formation, as also confirmed in this study.
4) The formation of branched cracks in the surface skin of the transition slab is related only with the lower pulling rate at the beginning, mainly due to a combination of adverse morphology and particle size based on microalloying elements, as well as the presence of Fe_3C and increased local segregation of harmful impurities.

ACKNOWLEDGEMENTS

This work was supported by project No.1/0387/11 of the Scientific Grant Agency of the Ministry of Education of the Slovak Republic and the Slovak Academy of Sciences and partly due to the project "European Community's Seventh Framework Programme (FP7/2007-2013) under grant agreement n° 312284., DESY proposal n° I-20120037 EC".

REFERENCES

[1] ROY, S., et al.: Prediction of Inhomogeneous Distribution of Microalloy Precipitates in Continuous-Cast High-Strength, Low-Alloy Steel Slab, Metallurgical and Materials Transactions A, Vol. 43A, 2012, pp.1845-1860.

[2] ROY, S., et al.: Austenite Grain Structures in Ti- and Nb-Containing High-Strength Low-Alloy Steel During Slab Reheating, Metallurgical and Materials Transactions A, published online: 17 October 2012.

[3] LUDLOW, V., et al.: Understanding the Role of Microalloy Precipitates in the Surface Cracking of Continuously Cast Slab, Acta Metallurgica Slovaca, Vol.13, 2007, pp.48-57.

[4] BEKEČ, P., et al.: Background of branched crack formation in surface zone of continuously-cast Ti-Nb microalloyed steel slab. In: COMAT 2014 Recent trends in structural materials, 3rd International Conference, 19-21 November 2014, Plzeň, Tanger Ltd., www.COMAT.cz, ISBN 978-80-87294-45-1.

[5] LONGAUEROVÁ, M., et al.: Influence of cooling rate on TiNb microalloyed steel slab surface zone fracture morphology, In: Acta Metallurgica Slovaca - Conference, Vol.3, 2013, ISSN 1338-1660, pp.30-39.